J. Ocean Univ. China (Oceanic and Coastal Sea Research)
https://doi.org/10.1007/s11802-018-3385-1
ISSN 1672-5182, 2018 17 (3): 609-613
http://www.ouc.edu.cn/xbywb/
E-mail:xbywb@ouc.edu.cn

DFT and 3D-QSAR Studies of Anti-Cancer Agents m-(4-Morpholinoquinazolin-2-yl) Benzamide Derivatives for Novel Compounds Design

ZHAO Siqi, ZHANG Guanglong, XIA Shuwei*, and YU Liangmin

Key Laboratory of Marine Chemistry Theory and Technology, *Ministry of Education*, *College of Chemistry and Chemical Engineering*, *Ocean University of China*, *Qingdao* 266100, *China*

(Received December 13, 2016; revised March 6, 2017; accepted October 20, 2017)

Abstract As a group of diversified frameworks, quinazolin derivatives displayed a broad field of biological functions, especially as anticancer. To investigate the quantitative structure-activity relationship, 3D-QSAR models were generated with 24 quinazolin scaffold molecules. The experimental and predicted pIC50 values for both training and test set compounds showed good correlation, which proved the robustness and reliability of the generated QSAR models. The most effective CoMFA and CoMSIA were obtained with correlation coefficient r^2_{ncv} of 1.00 (both) and leave-one-out coefficient q^2 of 0.61 and 0.59, respectively. The predictive abilities of CoMFA and CoMSIA were quite good with the predictive correlation coefficients (r^2_{pred}) of 0.97 and 0.91. In addition, the statistic results of CoMFA and CoMSIA were used to design new quinazolin molecules.

Key words quinazolin derivatives; anticancer; 3D-QSAR; electronic structure; molecular design

1 Introduction

Cancer is one of the most serious health problems in the world (Mohamed *et al*., 2016). Quinazolin derivatives has been regarded as effective drug scaffolds (Antoszczak *et al*., 2014) in cancer treatment (Alafeefy *et al*., 2008; Zhang *et al*., 2013) since their high-potency, low toxicity and diversity of substituent. Morpholino quinazolin derivatives have been proved carrying the good anticancer activities through docking studies, however, electronic structure and QSAR studies have been barely reported. Castillo *et al*. (2012) had studied a series of quinazolin derivatives using DFT method, the results showed that the presence of chlorine helped increasing the molecular reactivity. Hammond *et al*. (2003) reported a kind of potent inhibitor (KF24345) which showed less species heterogeneity than prototypical inhibitor NBMPR. Thus, it is need to carry out quantum chemistry and QSAR studies on quinazolin molecules to better understand the relationship between electronic structure and biological activity of this kind compound.

3D-QSAR models are also applied to design new useful compounds, sieve large beneficial active chemicals and further understand the mechanism (Joshi *et al*., 2014). In this paper, DFT calculations were used to explore the active sites of quinazolin molecules. 3D-QSAR of quinazolin derivatives and their electronic structures were also investigated in details. Finally, the results from CoMFA, CoMSIA and DFT were used as a guide in designing new quinazolin compounds.

2 Materials and Methods

Structures of quinazolin derivatives were optimized by DFT B3LYP/6-31G(d,p) Gaussian 09 program. QSAR study including parameter calculation and analysis for CoMFA and CoMSIA were performed by SYBYL-X2.0.

2.1 Data Set

In this paper, a series of 24 m-(4-morpholinoquinazolin-2-yl) benzamides (Wang *et al*., 2015) were used for 3D QSAR study. The pIC50 (-logIC50) values against HCT- 116 cell lines were listed in Table 1. The whole 3D structures were divided into two parts, structure A and structure B, based on their infrastructure. All molecules were randomly separated into two sets, training set and test set. The training set including 19 molecules was used to generate model. And the remaining 5 compounds were used as test set to verify the quality of predictive ability of generated model.

2.2 Molecular Alignment

All QSAR modeling studies including molecular align-

*Corresponding author. Tel: 0086-532-66782407
E-mail: shuweixia@ouc.edu.cn

Table 1 Structures, experimental and predicted pIC50 values for both training and test compounds

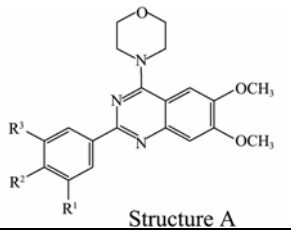

Structure A

No.	R^1	R^2	R^3	Exp pIC50	Pred pIC50	
					CoMFA	CoMSIA
1	$CONH_2$	H	H	6.05	6.04	6.03
2*	$CONH_2$	OCH_3	H	6.33	6.30	6.24
3	$CONH_2$	Cl	H	5.53	5.53	5.53
4	$CONH_2$	H	OCH_3	6.35	6.35	6.35
5	$CONH_2$	H	OBn	5.42	5.42	5.42
6	$CONH_2$	OBn	H	6.05	5.30	5.30
7	$CONH_2$	H	OH	6.06	6.07	6.08
8	$CONH_2$	OH	H	5.56	5.55	5.56
9	$CONH_2$	H	CF_3	6.15	6.15	6.16
10	$CONH_2$	H	OCF_3	6.52	6.52	6.51
11	CO_2CH_3	H	H	5.97	5.96	5.96
12	$CONHCH_3$	H	H	5.60	5.60	5.60
13	NHAc	H	H	5.85	5.86	5.85
14*	H	$CONH_2$	H	5.90	5.94	5.96
15	H	NHAc	H	5.96	5.97	5.95

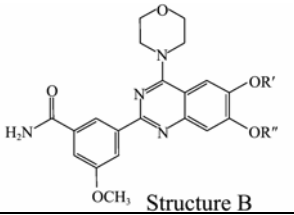

Structure B

No.	R’	R”	Exp pIC50	Pred pIC50	
				CoMFA	CoMSIA
16*	$CH_2CH_2OCH_3$	CH_3	6.05	6.04	6.24
17	$CH_2CH_2OCH_3$	$CH_2CH_2OCH_3$	5.04	5.05	5.05
18	CH_3	Bn	5.19	5.19	5.19
19*	CH_3	$CH_2CH_2OCH_3$	5.57	5.53	5.59
20	CH_3		5.5	5.49	5.49
21*	CH_3		5.89	5.78	5.85
22	CH_3	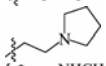	6.09	6.09	6.09
23	CH_3	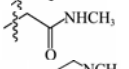	5.02	5.01	5.02
24	CH_3	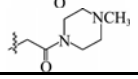	4.66	4.66	4.66

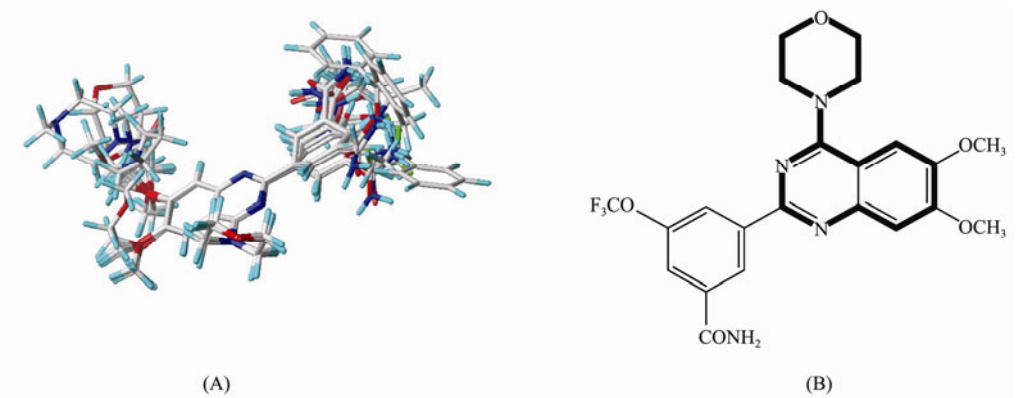

(A) (B)

Fig.1 Three-dimensional training set alignment (A) setting on a template molecule (B) (core structure for alignment is shown in bold and partial atoms are shown their label for further discussion).

ments were carried out using SYBYL-X2.0 without extra-defined values. Generally, low energy conformation of the highest bio-active molecule was set as reference. Thus, all molecules were aligned on Compound 10 (the most active compound) based on a common core. The aligned database and the template molecule were showed in Fig.1.

2.3 CoMFA Analysis

The grid spacing was set to 2.0Å each in all Cartesian directions. The CoMFA grid points generated with Tripos force field using a sp^3 carbon with net^{+1} charge. The maximum energy cutoff of steric and electrostatic fields was set to 30 kcal mol^{-1} (Lokwani *et al*., 2014).

2.4 CoMSIA Analysis

In CoMSIA study, the attenuation factor was set to 0.328. The grid spacing in CoMSIA calculations was same to CoMFA. Similarity indices were calculated between a probe and each atom of the molecules based on a Gaussian distance function (Zhang *et al*., 2016).

3 Results and Discussion

3.1 Frontier Orbital Analysis

According to the frontier molecular orbital theory, the highest occupied molecular orbital (HOMO) and the lowest unoccupied molecular orbital (LUMO) were important factors for bioactivity. The frontier molecular orbital diagrams of the most active molecule (compound 10) were showed in Fig.2. The HOMO of compound 10 is mainly constituted by morpholino, quinazolin and benzene rings; while LUMO is quinazolin and benzene rings. Similarly, HOMO-1 and LUMO+1 orbitals were then mainly distributed on aromatic and heteroatomic rings. HOMO/LUMO distribute over the basic skeleton of compound 10 but not over the substituent groups, which meant that morpholino, quinazolin should be functional sites of the molecule. It was the morpholino, quinazolin rings in all molecules that played a dominant role for the biological activity against HCT-116 cell lines. And the active parts could be used as common core in 3D-QSAR studies.

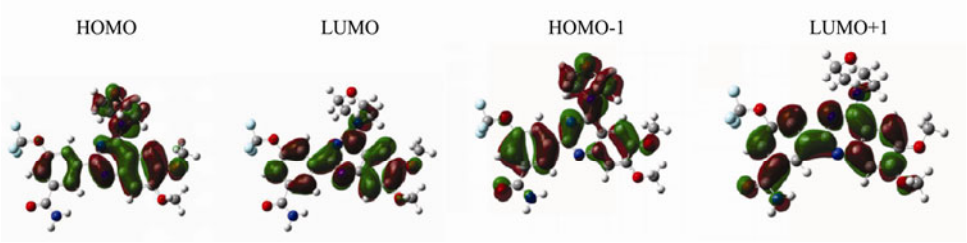

Fig.2 Frontier molecular orbital diagrams of compound 10.

3.2 CoMFA and CoMSIA Results

The results of CoMFA analysis on the contribution of steric and electrostatic fields were listed in Table 2. The most effective CoMFA and CoMSIA were obtained with correlation coefficient of 1.00 (both) and leave-one-out coefficient q^2 of 0.61 and 0.59, respectively. The predictive abilities of CoMFA and CoMSIA were quite good with the predictive correlation coefficients (r^2_{ncv}) of 0.97 and 0.91. In addition, the statistic results of CoMFA and CoMSIA were used to design new quinazolin molecules.

Table 2 Statistical results of CoMFA and CoMSIA models

Statistical parameter	CoMFA model	CoMSIA model
N	9	9
q^2	0.61	0.59
$r_{ncv}{}^2$	1.00	1.00
$r_{pred}{}^2$	0.97	0.91
SEE	0.01	0.01
F value	7794.17	4461.92
r^2 for test set	0.96	0.80
$Q_{F1}{}^2$	0.97	0.91
$Q_{F2}{}^2$	0.95	0.83
$Q_{F3}{}^2$	0.89	0.66
CCC	0.92	0.89

3.3 Contour Maps Analysis

Both contour maps of CoMFA and CoMSIA statistical results were interpreted using STDEV*COEFF type of field at 3D grid orientation for proper visualization. In this study, contour maps of CoMFA were displayed at steric and electrostatic fields in Fig.3. In CoMSIA model, contour maps of steric (S) and hydrophobic (H) were showed in Fig.4. All contour maps were consisted of 80% favorable and 20% unfavorable sites.

3.3.1 CoMFA map analysis

The compound 10 (pIC50 = 6.52) with the CoMFA model of steric contour map was shown in Fig.3A. The green contours represented the contribution of a high steric tendency, while yellow contours represented low steric tendency. In Fig.3A, two green contours were covering -OCF_3 (R^3 in structure A), which indicated bulky substitutions in R^3 position would increase the activity. Three yellow-color and green-color contour maps were overlapped at -$CONH_2$ (R^1 in structure A). That represented bulky-sized groups in R^1 would decrease the activity, but the size of the groups could not be infinitely small. In addition, two small steric favorable contour maps were observed over -OCH_3 (R" in structure B) at the terminal of quinazolin ring suggesting that bulky groups in this region would favor the activity. The electrostatic contour maps of compound 10 in CoMFA model was shown in Fig.3B. In Fig.3B, electrostatic field was expressed by blue contours for more positive charge groups and red for

more negative charge groups, respectively. In this figure, three large red contours were overlapping R^3 region at the terminal of benzene ring, which indicated high electrostatic groups would increase activity. Furthermore, two electropositive blue contours were overlapping R^1 region, showed positively charged groups at this position would increase activity.

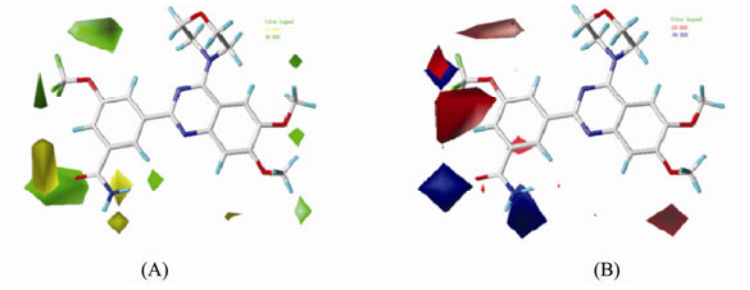

Fig.3 Steric (A) and Electrostatic (B) contour maps of the CoMFA model of compound 10.

3.3.2 CoMSIA map analysis

CoMSIA model contour maps of steric and hydrophobic fields were showed in Figs.4(A) and 4(B). CoMSIA contour maps at steric field of compound 10 showed the similar results to CoMFA model. So in this analysis, only hydrophobic field was discussed. Hydrophobic contour was indicated by cyan and purple colors representing hydrophobic and hydrophilic groups, respectively. In CoMSIA hydrophobic contour maps, one large cyan contour was covering the $-R^3$ group to benzene ring, while one large purple color and a small purple one overlapped at the same region. Based on the contribution of the contour map, it could be revealed hydrophilic groups in $-R^3$ region might enhance the activity, but the intensity of the hydrophilic property should not too strong. One hydrophilic favorable contour map was close to R^1 region, indicating hydrophilic favorable group at this region would increase the activity. Meanwhile, a small cyan-color contour map was overlapping at the terminal of the quinazolin ring, which indicated a small hydrophobic group in R" position could help with increasing activity.

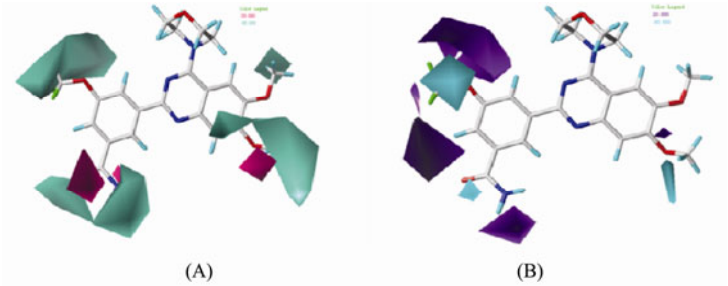

Fig.4 Steric (A) and Hydrophobic (B) contour maps of the CoMSIA model of compound 10.

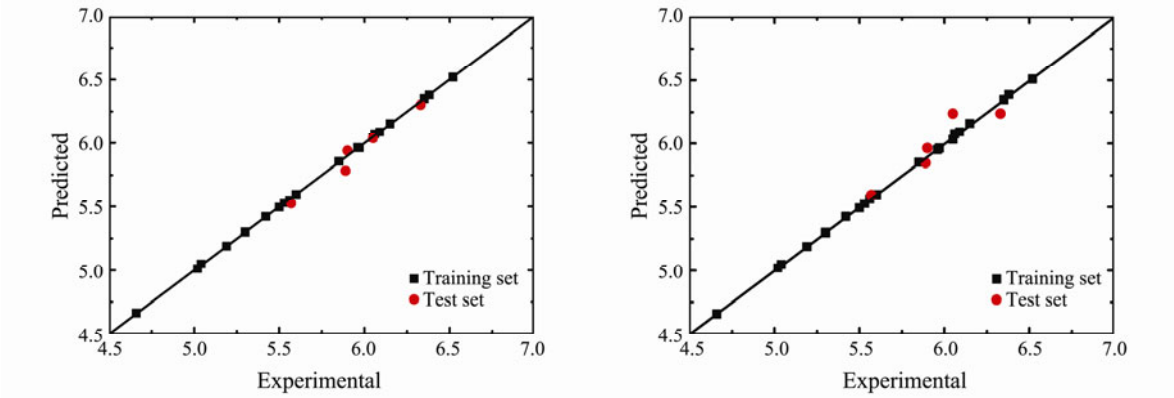

Fig.5 Plots of the experimental datum versus the predicted values of CoMFA (A) and CoMSIA (B) models.

3.4 External Test Set Validation

External test set validation is the most important part to test the predicted ability of the generated CoMFA and CoMSIA models. The $Q^2_{F_1}$, $Q^2_{F_2}$, $Q^2_{F_3}$ and the CCC value of external test set were listed in Table 2. The plot of predicted pIC50 value versus experimental pIC50 value of both training and test sets of CoMFA and CoMSIA models were presented in Fig.5. As results showed, the predictive activity values of training and test set were quite coincident with their experimental data respectively, which proved these build models for both CoMFA and

CoMSIA could be used to predict activity of novel designed molecules.

3.5 Designing Compounds

The designing information was obtained from the results of QSAR study relied on both CoMFA and CoMSIA. Contour map analysis showed structural requirements to be incorporated for increasing the activity by using less bulky and hydrophilic of R^2, more hydrophilic group and negative charge of R^3 and high electrostatic groups of R^1 (showed in Fig.6).

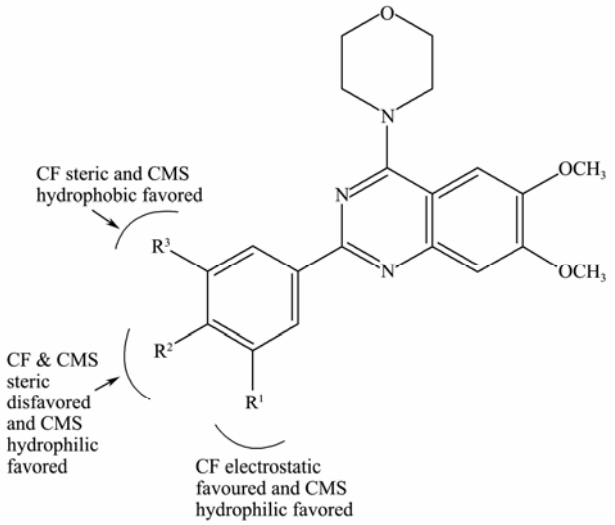

Fig.6 Structural requirements from CoMFA and CoMSIA for molecular design.

4 Conclusions

Aromatic and heteroatomic rings were the major skeletons of high bioactivity. Hence, quinazolin ring was considered to be a common core of the assignment step in 3D-QSAR studies. Great stability and predictive abilities of QSAR models on a series of 24 m-(4-morpholinoquinazolin-2-yl) benzamides were established. 3D Contour maps showed that several modifications on substituental groups would be beneficial for the promotion of the activity. Based on contour map analysis, improvement in activity has been achieved by substituting R^1, R^2 and R^3. This contributes majorly towards enhancing the original characters of molecules.

Acknowledgements

The authors would like to acknowledge financial supports from the National Natural Science Foundation of China (Nos. 50673085, 20677053), and the National High-Tech Research and Development Programme of China (No. 2010AA09Z203).

References

Alafeefy, A. M., Kadi, A. A., El-Azab, A. S., Abdel-Hamide, S. G., and Daba, M. Y., 2008. Synthesis, analgesic and anti-inflammatory evaluation of some new 3H-quinazolin-4-one derivatives. *Archiv Der Pharmazie*, **341**: 377-385.

Antoszczak, M., Maj, E., Napiórkowska, A., Stefańska, J., Augustynowicz-Kopeć, E., Wietrzyk, J., Janczak, J., Brzezinski, B., and Huczyński, A., 2014. Synthesis, anticancer and antibacterial activity of salinomycin N-Benzyl amides. *Molecules*, **19**: 19435-19459.

Hammond, J. R., and Archer, R. G. E., 2003. Interaction of the novel adenosine uptake inhibitor 3-[1-(6,7-Diethoxy-2- morpholinoquinazolin-4-yl)piperidin-4-yl]-1,6-dimethyl-2,4 (1H, 3H)-quinazolinedione Hydrochloride (KF24345) with the es and ei subtypes of equilibrative nucleoside transporters. *Journal of Pharmacology and Experimental Therapeutics*, **308**: 1083-1093.

Joshi, S. D., More, U. A., Aminabhavi, T. M., and Badiger, A. M., 2014. Two- and three-dimensional QSAR studies on a set of antimycobacterial pyrroles: CoMFA, Topomer CoMFA, and HQSAR. *Medicinal Chemistry Research*, **23**: 107-126.

Lokwani, D. K., Mokale, S. N., and Shinde, D. B., 2014. 3D QSAR studies based in silico screening of 4,5,6-triphenyl-1,2,3,4-tetrahydropyrimidine analogs for anti-inflammatory activity. *European Journal of Medicinal Chemistry*, **73**: 233-242.

Wang, X., Xin, M., Xu, J., Kang, B., Li, Y., Lu, S., and Zhang, S., 2015. Synthesis and antitumor activities evaluation of m-(4-morpholinoquinazolin-2-yl)benzamides *in vitro* and *in vivo*. *European Journal of Medicinal Chemistry*, **96**: 382-395.

Zhang, H., Hu, J., Zhao, J., and Zhang, Y., 2016. Spectrometric measurements and DFT studies on new complex of copper (II) with 2-((E)-9-ethyl-3-(2-(6-(4-methylpyridin-2-yl)pyridin-3-yl)vinyl)-9H-carbazole. *Spectrochimica Acta Part A: Molecular and Biomolecular Spectroscopy*, **168**: 78-85.

(Edited by Ji Dechun)